Stoichiometry of Ozonation of Environmentally Relevant Olefins in Saturated Hydrocarbon Solvents

ANTHONY L. GOMEZ, TANZA L. LEWIS, STACY A. WILKINSON, AND SERGEY A. NIZKORODOV*

Department of Chemistry, University of California, Irvine, California 92697-2025

The double bond-to-ozone reaction stoichiometry was quantified for ozonation of several environmentally relevant unsaturated fatty acids and monoterpenes in saturated hydrocarbon solvents. Olefins with initial concentrations from 30 μM to 3 mM were injected in a solvent (n-hexadecane, nonane, or cyclohexane) while an ozone-oxygen mixture was slowly bubbled through the solution. The number of ozone molecules consumed by the injection was quantified in the outgoing flow, and the expected 1:1 double bond-to-ozone reaction stoichiometry was observed only under subambient temperature conditions ($T < 250$ K). At room temperature, the effective number of double bonds oxidized by each ozone molecule increased to 2–5, with a higher degree of oxidation occurring at lower initial olefin concentrations. The observed enhancement in the stoichiometry is consistent with a competition between direct ozonation and free radical initiated oxidation of double bonds, with free radicals being produced by slow reactions between dissolved ozone and solvent molecules.

Introduction

Ozone is a criteria pollutant and is an important oxidant of unsaturated organics in indoor and outdoor air (*1, 2*). Typical mixing ratios of ozone in the lower atmosphere range from about 20–30 ppb (parts per billion by volume) in clean air to over 300 ppb in heavily polluted air. This results in lifetimes of atmospheric unsaturated organics, with respect to oxidation by ozone, ranging from minutes to days. Indoor ozone mixing ratios normally track the local outdoor ozone levels but are lower by a factor of 2–10 because of decomposition of ozone on various indoor surfaces (*1, 3*). However, alarmingly high levels of indoor ozone with mixing ratios well into the ppm (part per million by volume) range have been reported during building disinfection (*4*). Under these conditions, the rate and depth of oxidation of unsaturated organics increase considerably. To understand this chemistry in detail, oxidation of environmentally relevant organic films (*5–7*), organic aerosol particles (*8–11*), and various indoor materials (*4, 12–14*) by gas-phase ozone was investigated under a broad range of conditions.

The commonly accepted mechanism of ozonation of unsaturated organics (*15*) involves the cycloaddition of ozone to the double bond, followed by a rapid decomposition of the resulting primary ozonide into a highly reactive carbonyl oxide (Criegee intermediate) and a carbonyl. In solutions, stabilized carbonyl oxides undergo addition to carbonyls to form secondary ozonides, addition to alcohols, water, and carboxylic acids to form alkoxy-, hydroxy-, and acyloxy-hydroperoxides, respectively, and isomerization into carboxylic acids (*16*). In gas-phase ozonation reactions, carbonyl oxides may also undergo unimolecular decomposition to give OH radicals in fairly high yields (*17*).

It is often assumed that ozone reacts with unsaturated organics in a well-defined stoichiometric ratio, with one carbon–carbon double bond consumed per ozone molecule reacted. However, this work demonstrates that a single ozone molecule can effectively destroy several double bonds in dilute solutions of monoterpenes and unsaturated fatty acids via a chain reaction mechanism involving free radicals. This effect appears to be especially important near room temperature, and it may have significant implications for the environmental chemistry of ozone.

Furthermore, ozonation is frequently used in organic chemistry for synthesis of aldehydes and carboxylic acids from olefins. The reaction conditions are optimized for the maximal yield of the desired product; any deviations from the expected reaction stoichiometry are regarded as a nuisance. However, a recent study of ozonation of triptene reported 1.05–1.56:1 olefin-to-ozone stoichiometry for the complete triptene consumption and classified this result as "surprising" (*18*). Our work suggests that such a deviation from the 1:1 stoichiometry in ozonation of unsaturated organics may be a common effect and characterizes it for several environmentally relevant molecules.
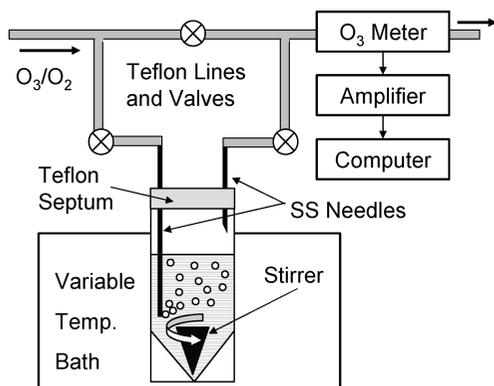
Experimental Section

Figure 1 shows a schematic diagram of the experimental setup used in this study. An oxygen flow of $F = 20$ sccm (standard cubic centimeters per second) containing ozone at a concentration of $[O_3] = 5 \times 10^{15}$ to 7×10^{16} molecules/cm^3 was bubbled into 5 mL of a stirred solvent contained in a 10 mL septum-sealed reaction vial immersed in a temperature-controlled bath. Solvents included n-hexadecane, n-nonane, cyclohexane, cyclopentane, and carbon tetrachloride. Purities and manufacturers for all chemicals used are specified in the Supporting Information. The concentration of ozone in the gas effluent was accurately measured with a calibrated home-built Hg-lamp photometer using base-*e* absorption cross-section of $\sigma_{253.65nm} = 1.136 \times 10^{-17}$ cm^2 (*19*).

Stock solutions of organic reactants in the same solvent were prepared and injected into the reaction vial in small volumes (1–150 μL) with a calibrated graduated syringe resulting in initial concentrations in the range of 30 μM to 3 mM. The reactants included unsaturated fatty acids (undecylenic, oleic, linoleic, and linolenic acids) and monoterpenes (α-pinene, β-pinene, and D-limonene). Successive injections were performed either with monotonically increasing reactant concentration or in a random order, with no difference in the results. To keep the ozone dissolution rate at constant levels, each experimental run was limited to a maximum of 10 injections. The solution remained clear and colorless after the injections, with no evidence of precipitation or colloid formation.

The reaction products were characterized by electrospray ionization mass-spectrometry (ESI-MS) in negative ion mode, which is especially sensitive to carboxylic acids. The mass-spectra confirmed that every injection of unsaturated fatty acid reactants resulted in a complete removal of the initial reactant from the mixture by O$_3$ and formation of a

* Corresponding author e-mail: nizkorod@uci.edu.

FIGURE 1. Experimental setup. An O_3/O_2 flow (20 sccm) is bubbled through a 10 mL reaction vial half-filled with a solvent, and $[O_3]$ is measured in the gas effluent. A small amount of olefin dissolved in the same solvent is periodically injected in the vial with a GC syringe.
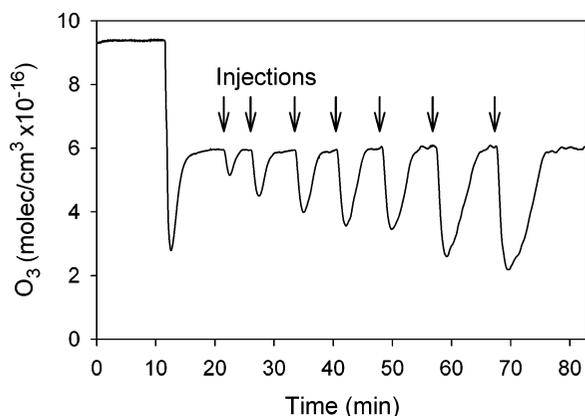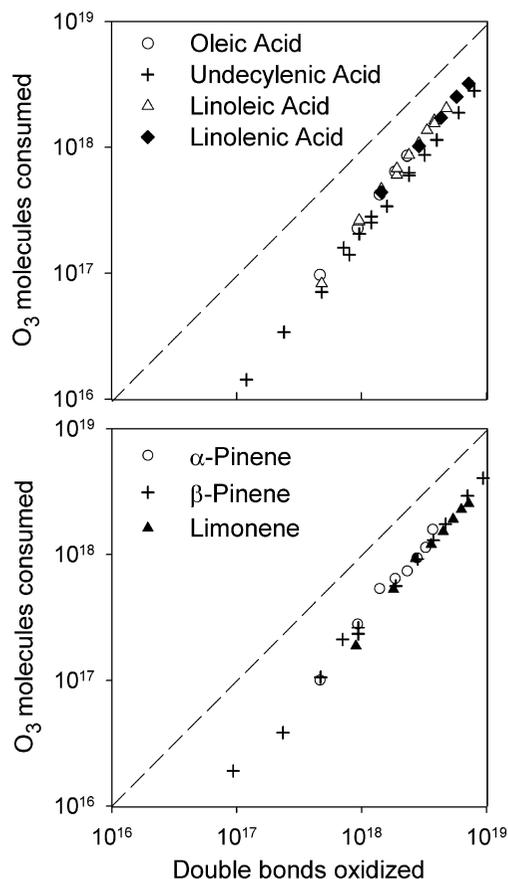

FIGURE 2. Sample experimental data. Ozone initially flows through the bypass, and is admitted into the reaction vial at $t = 11$ min. After a steady state is established, progressively increasing amounts of reactants are injected in the vial at times indicated by arrows. Each injection leads to a reduction in the effluent ozone concentration followed by a recovery to the steady state level.

FIGURE 3. Number of ozone molecules required to remove all double bonds in millimolar solutions of unsaturated fatty acids (top) and terpenes (bottom) in n-hexadecane at room temperature. The dashed line represents the expected 1:1 reaction stoichiometry. The horizontal axis is equal to the number of injected reactant molecules multiplied by the reactant's number of double bonds (three for linolenic acid, two for linoleic acid and D-limonene, and one for all other molecules).

complicated mixture of reaction products. In the case of monoterpene reactants, the removal of double bonds could not be explicitly verified because monoterpenes are not visible in ESI mass spectra, but it was assumed that the reaction was complete based on the similarity of oxidation conditions.

The degree of solvent oxidation was quantified in a separate set of experiments. Ozone was bubbled through the reaction vial filled with a pure solvent for 15–30 min using the setup shown in Figure 1. Cyclohexane and cyclopentane were used as solvents because they result in fewer possible ozonation products due to their increased molecular symmetry compared to the linear alkanes. After the ozone exposure, the solvent was injected into a GS/MS instrument as described in the Supporting Information. The yields of oxidation products (e.g., cyclohexanone and cyclohexanol in the case of cyclohexane) were measured with respect to the number of ozone molecules removed by the solution.
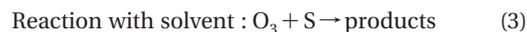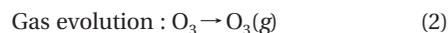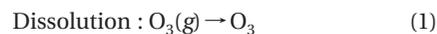
Results

Figure 2 shows a sample time-trace of ozone concentration in the gas effluent. When ozone was first admitted into the vial filled with neat solvent, its concentration plummeted because ozone started to displace the headspace air and

dissolve in the solution. After several minutes, a steady state was established with the ozone concentration in the outgoing flow reduced compared to that in the incoming flow. This reduction was attributed to ozone decomposition reactions that occurred in the solvent. A control experiment was performed in the absence of the solvent, which indicated that ozone surface losses in the reaction setup were small (<5%). The observed concentration reduction was typically 20−80%, depending on the solvent, temperature, and gas flow rate (for example, the reduction factor is $[O_3(g)]_{in}/[O_3(g)]_{out} = 1.6$ in Figure 2). The characteristic relaxation time for returning to the steady state (∼1 min) was comparable to but normally longer than the time scale for headspace gas-exchange (∼20 s = headspace volume/gas-flow rate).

This system can be approximately described in terms of the following competing processes;

$$\text{Dissolution} : O_3(g) \rightarrow O_3 \tag{1}$$

$$\text{Gas evolution} : O_3 \rightarrow O_3(g) \tag{2}$$

$$\text{Reaction with solvent} : O_3 + S \rightarrow \text{products} \tag{3}$$

O_3 refers to dissolved ozone, $O_3(g)$ refers to gas-phase ozone in the vial headspace, and S refers to solvent molecules. Under the steady state conditions, the rate of dissolution (1) is balanced by the combined rates of removal of ozone from solution by reactions 2 and 3.

Because of ozone's high reactivity, it is difficult to attain its true solubility equilibrium (20). Under the steady flow conditions used in this work, Henry's law is not expected to be obeyed because the decomposition of ozone in reaction 3 is significant on the time scales of headspace gas-exchange (~20 s) and gas-to-liquid mass transfer (~1 min). References 21 and 22 reported effective Ostwald coefficients (L = dimensionless ratio of ozone concentration in the solution to that in the gas phase) that were in the range of $L = 1.5-2.5$ for ozone bubbled through several organic solvents at room temperature. The Ostwald coefficients increased by about an order of magnitude at −78 °C. We similarly measured the concentration of dissolved ozone by bubbling it thought a UV/Vis spectrometer cell filled with cyclohexane. This resulted in $L \sim 1.0$ (with respect to the effluent gas-phase ozone concentration) for ozone dissolved in room-temperature cyclohexane, suggesting that the dissolved ozone concentration was limited by mass-transfer. However, this lack of complete solubility equilibrium is not going to affect the results and conclusions presented below.

Figure 2 shows that the measured concentration of ozone exiting the reaction vial dropped after each organic reactant (R) injection, and returned to the initial steady state value after the reaction was complete.

$$\text{Reaction with olefin}: O_3 + R \rightarrow \text{products} \quad (4)$$

For some injections, the initial concentration of dissolved ozone $[O_3]_0$ exceeded the initial concentration of reactant, $[R]_0$. Under these conditions, the reactant was promptly consumed (estimated $t_{1/2} < 1$ s), and the ozone concentration recovered on the time scale of re-establishing the dissolution/solvent decomposition steady state. In other cases, $[R]_0$ was larger than $[O_3]_0$, leading to a nearly complete dissolved ozone depletion and a longer steady state recovery time as reaction 4 continued to consume ozone supplied by dissolution 1 until all the reactant was consumed. This effect is clearly visible in Figure 2; the widths of the dips in ozone concentration increase with the amount of added reactant.

The absolute number of ozone molecules required to re-establish the steady state disrupted by reaction 4 was obtained by integrating the time-dependent ozone concentration for each injection (eq 5),

$$O_3 \text{ molecules consumed} =$$

$$F \times \int ([O_3(g)]_{ss} - [O_3(g)](t)) \, dt \quad (5)$$

where F is the O_3/O_2 flow rate in cm^3 s^{-1}, and $[O_3(g)]_{ss}$ is the steady state ozone concentration in the gas effluent in molecules cm^{-3}. Figure 2 demonstrates that $[O_3(g)]_{ss}$ remained constant over the course of the experiment, suggesting that the slow accumulation of reaction products in solution did not strongly affect the ozone dissolution/solvent decomposition rates. The absolute number of double bonds that reacted with ozone was calculated from the known reactant injection volumes and concentrations. The extent of double bond removal was explicitly verified by ESI-MS as described in the Experimental Section.

Figure 3 displays the number of ozone molecules consumed in reaction 4 as a function of the number of injected double bonds at room temperature. To calculate the latter, the number of injected reactant molecules was multiplied by the reactant's number of double bonds: three for linolenic acid, two for linoleic acid and D-limonene, and one for all other molecules. The dashed line corresponds to the expected stoichiometric 1:1 ozonation. Clearly, under these experimental conditions, consumption of one ozone molecule results in an elimination of more than one double bond. Deviations from the 1:1 double bond-to-ozone (DB:O$_3$) stoichiometry are noticeably larger at lower initial reactant
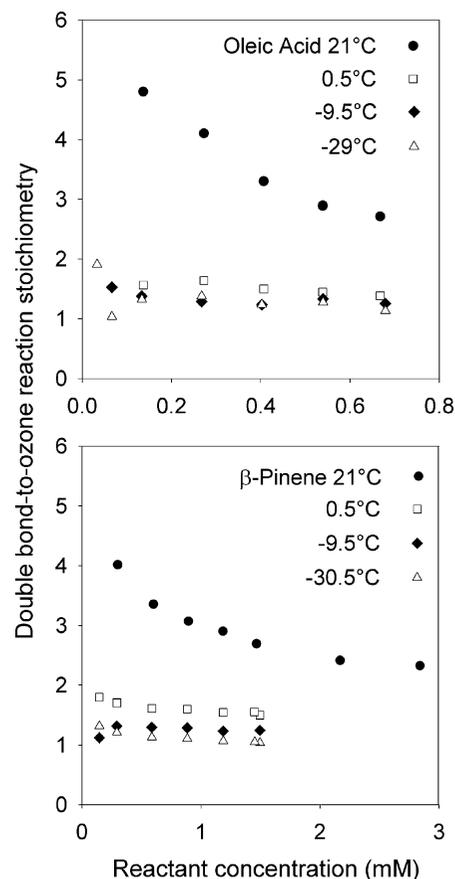
FIGURE 4. Temperature and concentration effects on the DB:O$_3$ stoichiometry for ozonation of oleic acid (top) and β-pinene (bottom). Positive and negative temperature measurements were done in n-hexadecane and n-nonane, respectively.

concentrations. However, the DB:O$_3$ ratio does not strongly depend on reactant's chemical nature; all reactants appear to fall on the same DB:O$_3$ curve, within the experimental uncertainty. Data in Figure 3 correspond to n-hexadecane solvent; DB:O$_3$ ratios measured in n-nonane were the same within the experimental uncertainty.

The average number of double bonds depleted by each ozone molecule is plotted against the reactant concentration in Figure 4 for several temperatures. The observed DB:O$_3$ ratio converges at the conventional value of 1:1 only at the highest concentrations and lowest temperatures used in this work. At room temperature, this ratio is about 2−3:1 at higher reactant concentrations, and it increases to 4−5:1 at lower concentrations. At lower temperatures, this effect is less dramatic, with the number of consumed double bonds approaching 1.5 at the lowest reactant concentrations.

Discussion

The standard Criegee mechanism of ozonation of olefins involves the cycloaddition of ozone across the double bond followed by a fast decomposition of the resulting primary ozonide (POZ) into a carbonyl and carbonyl oxide pair (15). The usual fate of carbonyl oxides in nonparticipating solvents is recombination with the geminate carbonyls yielding a secondary ozonide (SOZ) and resulting in DB:O$_3$ = 1:1 (Figure 5). SOZ was previously observed in room temperature ozonation of unsaturated fatty acids and triglycerides (8, 23−26). In the case of oleic acid, our ESI mass spectra of reaction products showed that SOZ (observed at $m/z = 2M_{SOZ} - 1$) was indeed an important product of ozonation of unsaturated fatty acids at low temperatures. However, the
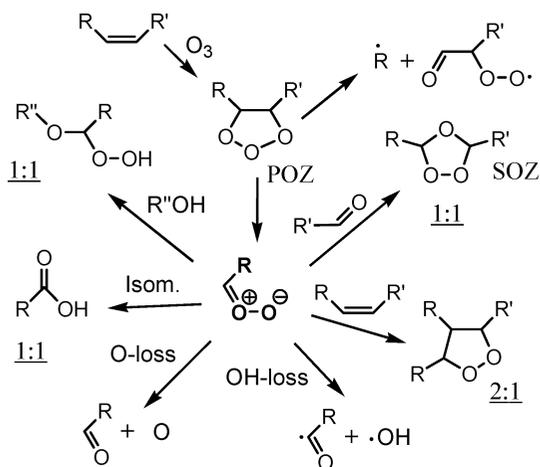
FIGURE 5. DB:O$_3$ stoichiometry for different reactions of carbonyl oxide: cycloaddition to a carbonyl (1:1), cycloaddition to a double bond (2:1), isomerization (1:1), and reaction with alcohols or carboxylic acids (1:1). OH-loss and O-loss are common in gas-phase ozonolysis but are less likely to occur in solution. Unconventional decomposition of POZ into alkyl and alkylperoxy radicals (shown in the upper right corner) was proposed in ref *29*.

number of product peaks in the ESI-MS spectra greatly increased, and the relative SOZ yield dropped considerably at room temperature. On the basis of the observed DB:O$_3$ ratio and of the ESI-MS data, we conclude that SOZ is not the dominant reaction pathway under room temperature conditions.

Direct cycloaddition of stabilized carbonyl oxides to double bonds could potentially result in 2:1 DB:O$_3$ stoichiometry. However, carbonyl oxides do not undergo cycloaddition to double bonds unless the latter are strongly polarized by substituent groups (*15, 16*). None of the reactants used in this work have such activated double bonds. Furthermore, recent work on ozonation of pure unsaturated fatty acids showed no evidence for such reactions (*8, 27, 28*).

With carboxylic acids used for reactants (undecylenic, oleic, linoleic, and linolenic acids), the carbonyl oxides are likely to add to carboxylic groups producing acyloxy-hydroperoxides. This is the dominant reaction pathway in ozonation of pure unsaturated fatty acids (*8, 23, 24, 27, 28*). Although these reactions will produce >1:1 reactant-to-ozone stoichiometry, the DB:O$_3$ stoichiometry will remain at 1:1 (Figure 5).
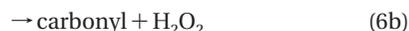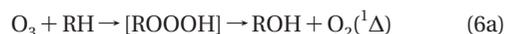
In summary, the observed DB:O$_3$ stoichiometry in a large excess of 1:1 is not consistent with known solution chemistry of stabilized carbonyl oxides. Additional reaction mechanisms are clearly involved in dilute solutions of olefins aerated with ozone/oxygen mixtures. We hypothesize that the excess double bonds are oxidized by free radicals, which are generated by one of the following mechanisms: (a) unimolecular decomposition of carbonyl oxides (*17*), (b) unconventional decomposition of POZ (*29*), or (c) autoxidation reactions between ozone and solvent molecules.

Unimolecular decomposition of carbonyl oxides into either OH and an alkyl radical or into an O-atom and carbonyl (Figure 5) are well-known pathways in gas-phase ozonation of olefins (*17*). Efficient decomposition into OH would provide an attractive explanation for the anomalous DB:O$_3$ stoichiometry because highly reactive OH can directly add to a double bond or abstract an H-atom from a solvent molecule, inducing a short chain reaction (see below). However, carbonyl oxide decomposition has not been previously observed in solutions. Given that the yield of OH in gas-phase decomposition of carbonyl oxides is reduced at high

pressures (*30–32*), this reaction is likely to be strongly suppressed in solution.
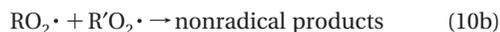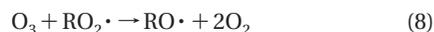
Pryor (*29*) examined the mechanism of free radical formation from reactions between ozone and olefins and demonstrated that there is an alternative pathway for POZ decomposition directly yielding an alkyl radical and alkyl peroxy radical (Figure 5). He estimated that about 10% of POZ molecules decompose in this way (with respect to the conventional carbonyl oxide + carbonyl channel) and result in lipid peroxidation in biological systems by radical induced mechanisms with chain lengths of 5–50.

Finally, free radicals may be produced without any added olefinic reactants by reaction 3 between ozone and solvent molecules. Indeed, ozone is known to slowly react with unactivated C–H bonds in saturated hydrocarbons (*33, 34*). It is believed that the reaction proceeds through a hydrotrioxide intermediate that decomposes into various reactive products (eqs 6a–c).

$$O_3 + RH \rightarrow [ROOOH] \rightarrow ROH + O_2(^1\Delta) \qquad (6a)$$

$$\rightarrow carbonyl + H_2O_2 \qquad (6b)$$

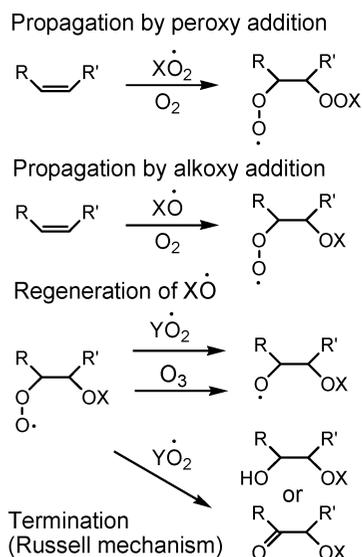$$\rightarrow RO\cdot + HO_2\cdot \qquad (6c)$$

To confirm that these reactions take place under our experimental conditions, we measured the yield of major stable products for the reaction between ozone and cyclohexane and between ozone and cyclopentane (see Supporting Information). For cyclohexane, the major products were cyclohexanol and cyclohexanone formed in a ratio of 3:1, in agreement with ref (*35*). The overall product yield (sum of all products/ozone molecules lost in solution) was close to 100% at room temperature. For cyclopentane, the dominant products were cyclopentanol and cyclopentanone. At room temperature, ozone was destroyed by both solvents with an effective reaction rate of $\sim10^{-5}$ mol L^{-1} s^{-1}, which corresponds to the rate constant of $\sim10^{-2}$ L mol^{-1} s^{-1} for reaction 3. For reference, literature values for the rate constant of O$_3$ + cyclohexane reaction in CCl$_4$ are 1.1×10^{-2} L mol^{-1} s^{-1} (*36*) and 3.1×10^{-2} L mol^{-1} s^{-1} (*37*). For cyclopentane, the measured reaction rate decreased by approximately an order of magnitude at −30 °C.

Reaction (6c) generates alkoxy (RO) and hydroperoxy (HO$_2$) radicals directly. Additional free radicals can be produced via secondary reactions such as the following.

$$O_3 + H_2O_2 \rightarrow OH\cdot + H_2O + O_2 \qquad (7)$$

$$O_3 + RO_2\cdot \rightarrow RO\cdot + 2O_2 \qquad (8)$$

$$RO\cdot + RH(+O_2) \rightarrow ROH + RO_2\cdot \qquad (9)$$

$$RO_2\cdot + R'O_2\cdot \rightarrow RO\cdot + R'O\cdot + O_2 \qquad (10a)$$

$$RO_2\cdot + R'O_2\cdot \rightarrow nonradical products \qquad (10b)$$

The reaction between ozone and hydrocarbon solvent, despite its low reaction rate, may produce sufficient concentrations of free radicals (alkyl, alkoxy, alkyl peroxy, OH, and HO$_2$) to initiate oxidation of injected olefinic reactants in competition with their direct ozonation by the Criegee mechanism. Indeed, the combined concentration of free radicals generated by reaction 3 (rate $\sim10^{-5}$ mol L^{-1} s^{-1}) and consumed in diffusion-limited radical–radical termination processes (rate constants $\sim10^9$ L mol^{-1} s^{-1}) can reach ~0.1 μM. Although this concentration is several orders of magnitude lower than the steady state concentration of dissolved ozone, it is compensated by larger rate constants for reactions between some of these free radicals and olefins, compared to ozone-olefin reactions. (For example, rate constants for reactions of cyclohexene with OH and O$_3$ are 8.8×10^9 L mol^{-1} s^{-1} and 2.2×10^6 L mol^{-1} s^{-1}, respectively (*38*).)

Propagation by peroxy addition

Propagation by alkoxy addition

Regeneration of XȮ

Termination
(Russell mechanism)

FIGURE 6. Possible chain reaction mechanism for oxidation of olefins resulting in DB:O$_3$ ratio in excess of 1:1. X, Y = H or alkyl.

We attempted to differentiate between the three possible mechanisms of free radical production (carbonyl oxide decomposition, POZ decomposition, and ozone + solvent reactions) by measuring the DB:O$_3$ ratio in different kinds of solvents. Results of these measurements are given in the Supporting Information. Room temperature ozonation of undecylenic acid in CCl$_4$, which is highly inert toward ozone at room temperature, resulted in DB:O$_3$ = 1.4(1):1 with no dependence on the initial reactant's concentration (0.2–2.0 mM). On the contrary, ozonation of oleic acid in methanol or a methanol/acetic acid mixture, participating solvents known to efficiently scavenge carbonyl oxides (15), resulted in DB:O$_3$ in excess of 10:1 and a strong dependence on the initial reactant concentration (see Figure 1S in the Supporting Information). High DB:O$_3$ ratios observed in participating solvents are not consistent with the carbonyl oxide decomposition mechanism. The lack of anomalous reaction stoichiometry in CCl$_4$ strongly suggests that reactions between ozone and saturated hydrocarbon solvents act as the free radical sources. However, the observed deviation from DB:O$_3$ = 1:1 in CCl$_4$ does not rule out the mechanisms involving POZ and carbonyl oxide decomposition. More sophisticated experiments are necessary to distinguish between the mechanisms with more certainty.

Regardless of the mechanism of their generation, free radicals are likely to increase the observed DB:O$_3$ stoichiometry above the 1:1 level expected for a normal ozonation (Figure 6). Alkylperoxy radicals RO$_2$ are known to directly add to double bonds and to induce polymerization in certain readily polymerizable olefins (39). They can also be converted into more reactive alkoxy radicals RO by reaction with ozone (eq 8) or with another alkylperoxy radical (eq 10a). Kinetic information on reactions of alkoxy radicals with olefins is limited, but they are likely to undergo addition to double bonds with appreciable rates (40). Addition of RO or RO$_2$ to a double bond will be immediately followed by the addition of O$_2$ to the resulting radical to form a new alkylperoxy radical (Figure 6), which will propagate the chain further. The most likely termination step in this mechanism is reaction between two alkylperoxy radicals (eq 10b) giving stable carbonyl and alcohol via the Russell mechanism (39). This termination step is consistent with our observation that lower concentrations of reactants result in larger DB:O$_3$ ratios.

A large number of research groups have studied ozonolysis of oleic acid as a model for oxidative aging of atmospheric organic material (6–8, 10, 11, 24, 28, 41–44). In these studies, highly concentrated or pure oleic acid is exposed to relatively low gas-phase ozone concentrations (<1 ppm). Although we were unable to reliably measure the reaction stoichiometry for concentrated solutions of reactants, the concentration dependence in Figure 4 suggests that DB:O$_3$ should approach the expected limit of 1:1 for pure reactants. Under these conditions, direct oxidation of double bonds by ozone is the dominant pathway, and generation of free radicals by oxidation of saturated carbon atoms in oleic acid via reaction 3 can be ignored. However, the chain reaction mechanism discussed above may become important in more realistic organic aerosol, where unsaturated organics is considerably diluted with less reactive saturated organics.

A highly questionable disinfection method that involves treatment of indoor surfaces with high concentrations of gas-phase ozone is increasingly used by the hotel industry and residential cleaning services (4). The common practice is to operate one or several powerful ozone generators in a closed room for several hours under ambient temperature and humidity conditions. The steady state ozone concentrations reached during the disinfection can be in the hundreds of ppm range, that is, approaching the concentrations used in this work. In addition to decomposition on dry indoor surfaces such as carpets (13, 45), ozone may dissolve in aqueous and organic surface films and partly oxidize the content of these films via solution phase chemistry. We stress that cleaning of indoor surfaces by gas-phase ozone is a highly ineffective process because of low reaction rates between ozone and saturated organics (1). Indeed, even at 100 ppm ozone mixing ratio in indoor air, it takes hundreds of hours for ozone partitioned in an organic surface film to oxidize the first CH bond in a typical linear paraffin molecule.

The main implication of this work is that oxidation of unsaturated organic materials in the organic surface films is likely to be driven by secondary products of reactions between ozone and solvent molecules and not simply by direct ozonation. Involvement of free radicals in the process results in a much more complicated set of products compared to the classic Criegee mechanism of olefin ozonation. This may have implication for the assessment of health effects of organic products of indoor ozone chemistry, which may in fact be more harmful than ozone itself (46).

Supporting Information Available
This section contains information on chemicals used, DB:O$_3$ ratios measured in nonhydrocarbon solvents, and description of GC/MS measurements. This information is available free of charge via the Internet at http://pubs.acs.org.

Literature Cited
(1) Weschler, C. J. Ozone in indoor environments: Concentration and chemistry. *Indoor Air* **2000**, *10*, 269–288.
(2) Atkinson, R.; Carter, W. P. L. Kinetics and mechanisms of the gas-phase reactions of ozone with organic compounds under atmospheric conditions. *Chem. Rev.* **1984**, *84*, 437–470.
(3) Sabersky, R. H.; Sinema, D. A.; Shair, F. H. Concentrations, decay rates, and removal of ozone and their relation to establishing clean indoor air. *Environ. Sci. Technol.* **1973**, *7*, 347–353.
(4) Poppendieck, D.; Hubbard, H.; Ward, M.; Weschler, C.; Corsi, R. L. Ozone reactions with indoor materials during building disinfection. *Atmos. Environ.* **2007**, *41*, 3166–3176.
(5) Eliason, T. L.; Aloisio, S.; Donaldson, D. J.; Cziczo, D. J.; Vaida, V. Processing of unsaturated organic acid films and aerosols by ozone. *Atmos. Environ.* **2003**, *37*, 2207–2219.

(6) Asad, A.; Mmereki, B. T.; Donaldson, D. J. Enhanced uptake of water by oxidatively processed oleic acid. *Atm. Chem. Phys.* **2004**, *4*, 2083–2089.

(7) Knopf, D. A.; Anthony, L. M.; Bertram, A. K. Reactive uptake of O_3 by multicomponent and multiphase mixtures containing oleic acid. *J. Phys. Chem. A* **2005**, *109*, 5579–5589.

(8) Ziemann, P. J. Aerosol products, mechanisms, and kinetics of heterogeneous reactions of ozone with oleic acid in pure and mixed particles. *Faraday Discuss.* **2005**, *130*, 469–490.

(9) Hearn, J. D.; Smith, G. D. Measuring rates of reaction in supercooled organic particles with implications for atmospheric aerosol. *Phys. Chem. Chem. Phys.* **2005**, *7*, 2549–2551.

(10) Katrib, Y.; Martin, S. T.; Hung, H.-M.; Rudich, Y.; Zhang, H.; Slowik, J. G.; Davidovits, P.; Jayne, J. T.; Worsnop, D. R. Products and mechanisms of ozone reactions with oleic acid for aerosol particles having core-shell morphologies. *J. Phys. Chem. A* **2004**, *108*, 6686–6695.

(11) Smith, G. D.; Woods, E. III.; DeForest, C. L.; Baer, T.; Miller, R. E. Reactive uptake of ozone by oleic acid aerosol particles: Application of single-particle mass spectrometry to heterogeneous reaction kinetics. *J. Phys. Chem. A* **2002**, *106*, 8085–8095.

(12) Grontoft, T.; Raychaudhuri, M. R. Compilation of tables of surface deposition velocities for O_3, NO_2 and SO_2 to a range of indoor surfaces. *Atmos. Environ.* **2004**, *38*, 533–544.

(13) Morrison, G. C.; Nazaroff, W. W. The rate of ozone uptake on carpets: Experimental studies. *Environ. Sci. Technol.* **2000**, *34*, 4963–4968.

(14) Moriske, H.-J.; Ebert, G.; Konieczny, L.; Menk, G. Concentrations and decay rates of ozone in indoor air in dependence on building and surface materials. *Toxicol. Lett.* **1998**, *96,97*, 319–323.

(15) Bailey P. S. *Organic Chemistry*, Part 1: Ozonation in Organic Chemistry, Vol 1: Olefinic Compounds; Academic Press: New York/London, 1978; Vol *39*.

(16) Bunnelle, W. H. Preparation, properties, and reactions of carbonyl oxides. *Chem. Rev.* **1991**, *91*, 335–362.

(17) Paulson, S. E.; Chung, M. Y.; Hasson, A. S. OH radical formation from gas-phase reaction of ozone with terminal alkenes and the relationship between structure and mechanism. *J. Phys. Chem. A* **1999**, *103*, 8125–8138.

(18) Schank, K.; Marson, C.; Heisel, T.; Martens, K.; Wagner, C. Surprising results during the re-investigation of the formation and decomposition of triptene ozonide. *Helv. Chim. Acta* **2000**, *83*, 3312–3332.

(19) Mauersberger, K.; Hanson, D.; Barnes, J.; Morton, J. Ozone vapor pressure and absorption cross-section measurements: Introduction of an ozone standard. *J. Geophys. Res. D* **1987**, *92*, 8480.

(20) Solubility data series. In *Oxygen and Ozone*, Battino, R. Ed.; Pergamon Press: Oxford/New York, 1981; Vol *7*.

(21) Tarunin, B. I.; Perepletchikov, M. L.; Aleksandrov, Y. A. Solubility of ozone in some liquid organic compounds. *Z. Obshchei Khim.* **1982**, *52*, 478–481.

(22) Aleksandrov, Y. A.; Tarunin, B. I.; Perepletchikov, M. L. Solubility of ozone in some liquid individual compounds and their mixtures. *Z. Obshchei Khim.* **1976**, *46*, 3–5.

(23) Mochida, M.; Katrib, Y.; Jayne, J. T.; Worsnop, D. R.; Martin, S. T. The relative importance of competing pathways for the formation of high-molecular-weight peroxides in the ozonolysis of organic aerosol particles. *Atm. Chem. Phys.* **2007**, *6*, 4851–4866.

(24) Zahardis, J.; Petrucci, G. A. The oleic acid-ozone heterogeneous reaction system: Products, kinetics, secondary chemistry, and atmospheric implications of a model system — A review. *Atm. Chem. Phys.* **2007**, *7*, 1237–1274.

(25) Lai, C. C.; Finlayson-Pitts, B. J.; Willis, W. V. Formation of secondary ozonides from the reaction of an unsaturated phosphatidylcholine with ozone. *Chem. Res. Toxicol.* **1990**, *3*, 517–523.

(26) Lai, C. C.; Yang, S. H.; Finlayson-Pitts, B. J. Interactions of monolayers of unsaturated phosphocholines with ozone at the air-water interface. *Langmuir* **1994**, *10*, 4637–4644.

(27) Gomez, A.; Park, J.; Walser, M.; Lin, A.; Nizkorodov, S. A. UV photodissociation spectroscopy of oxidized undecylenic acid films. *J. Phys. Chem. A* **2006**, *110*, 3584–3592.

(28) Hearn, J. D.; Lovett, A. J.; Smith, G. D. Ozonolysis of oleic acid particles: Evidence for a surface reaction and secondary reactions involving Criegee intermediates. *Phys. Chem. Chem. Phys.* **2005**, *7*, 501–511.

(29) Pryor, W. A. Mechanisms of radical formation from reactions of ozone with target molecules in the lung. *Free Radical Biol. Med.* **1994**, *17*, 451–465.

(30) Presto, A. A.; Donahue, N. M. Ozonolysis fragment quenching by nitrate formation: The pressure dependence of prompt OH radical formation. *J. Phys. Chem. A* **2004**, *108*, 9096–9104.

(31) Kroll, J. H.; Clarke, J. S.; Donahue, N. M.; Anderson, J. G.; Demerjian, K. L. Mechanism of HO_x formation in the gas-phase ozone-alkene reaction. 1. Direct, pressure-dependent measurements of prompt OH yields. *J. Phys. Chem. A* **2001**, *105*, 1554–1560.

(32) Fenske, J. D.; Hasson, A. S.; Paulson, S. E.; Kuwata, K. T.; Ho, A.; Houk, K. N. The pressure dependence of the OH radical yield from ozone-alkene reactions. *J. Phys. Chem. A* **2000**, *104*, 7821–7833.

(33) Bailey P. S. Organic Chemistry Part 2: Ozonation in organic chemistry, Vol 2: Nonolefinic compounds; Academic Press: New York/London, 1982; Vol *39*.

(34) Nangia, P. S.; Benson, S. W. Thermochemistry and kinetics of ozonation reactions. *J. Am. Chem. Soc.* **1980**, *102*, 3105–3115.

(35) Hamilton, G. A.; Ribner, B. S.; Hellman, T. M. Mechanism of alkane oxidation by ozone. *Adv. Chem. Ser.* **1968**, *77*, 15–25.

(36) Williamson, D. G.; Cvetanovic, R. J. Rates of ozone-paraffin reactions in carbon tetrachloride solution. *J. Am. Chem. Soc.* **1970**, *92*, 2949–2952.

(37) Kurz, M. E.; Pryor, W. A. Radical production from the interaction of closed-shell molecules. 9. Reaction of ozone with tert-butyl hydroperoxide. *J. Am. Chem. Soc.* **1978**, *100*, 7953–7959.

(38) Neta, P.; Huie, R. E.; Ross, A. B. Rate constants for reactions of inorganic radicals in aqueous solution. *J. Phys. Chem. Ref. Data* **1988**, *17*, 1027–1284.

(39) Ingold, K. U. Peroxy radicals. *Acc. Chem. Res.* **1969**, *2*, 1–9.

(40) Gomez, N.; Henon, E.; Bohr, F.; Devolder, P. Rate constants for the reactions of CH_3O with cyclohexane, cyclohexene, and 1,4-cyclohexadiene: variable temperature experiments and theoretical comparison of addition and H-abstraction channels. *J. Phys. Chem. A* **2001**, *105*, 11204–11211.

(41) Morris, J. W.; Davidovits, P.; Jayne, J. T.; Jimenez, J. L.; Shi, Q.; Kolb, C. E.; Worsnop, D. R.; Barney, W. S.; Cass, G. Kinetics of submicron oleic acid aerosols with ozone: A novel aerosol mass spectrometric technique. *Geophys. Res. Lett.* **2002**, *29*, 71/71–71/74.

(42) Hung, H.-M.; Katrib, Y.; Martin, S. T. Products and mechanisms of the reaction of oleic acid with ozone and nitrate radical. *J. Phys. Chem. A* **2005**, *109*, 4517–4530.

(43) Hung, H.-M.; Ariya, P. Oxidation of oleic acid and oleic acid/sodium chloride(aq) mixture droplets with ozone: Changes of hygroscopicity and role of secondary reactions. *J. Phys. Chem. A* **2007**, *111*, 620–632.

(44) Katrib, Y.; Biskos, G.; Buseck, P. R.; Davidovits, P.; Jayne, J. T.; Mochida, M.; Wise, M. E.; Worsnop, D. R.; Martin, S. T. Ozonolysis of mixed oleic-acid/stearic-acid particles: reaction kinetics and chemical morphology. *J. Phys. Chem. A* **2005**, *109*, 10910–10919.

(45) Weschler, C. J.; Hodgson, A. T.; Wooley, J. D. Indoor chemistry: ozone, volatile organic compounds, and carpets. *Environ. Sci. Technol.* **1992**, *26*, 2371–2377.

(46) Weschler, C. J. Ozone's impact on public health: Contributions from indoor exposures to ozone and products of ozone-initiated chemistry. *Envir. Health Persp.* **2006**, *114*, 1489–1496.